Organometallic Chemistry

Protonation of ferrocene, ruthenocene, and osmocene: a density functional study

Yu. A. Borisov and N. A. Ustynyuk*

A. N. Nesmeyanov Institute of Organoelement Compounds, Russian Academy of Sciences, 28 ul. Vavilova, 119991 Moscow, Russian Federation.
Fax: +7 (095) 135 5085. E-mails: yabor@ineos.ac.ru; ustynyuk@ineos.ac.ru

Protonated forms of the ferrocene, ruthenocene, and osmocene molecules in the gas phase were calculated using the density functional approach with the Becke—Lee—Young—Parr functional. The proton affinity energies of ferrocene, ruthenocene, and osmocene were estimated at 214.2, 220.3, and 229.7 kcal mol^{-1}, respectively. The addition of a proton to carbon atoms of the cyclopentadienyl ring in the ferrocene molecule and to the metal atom in the ruthenocene and osmocene molecules is more energetically favorable. No minimum corresponding to ring protonation was located on the potential energy surface of protonated osmocene. The C—H_{endo} bond in the ring-protonated $[C_{10}H_{11}M]^+$ (M = Fe, Ru) cations is involved in agostic interaction with the metal atom. Transition states of interconversions between the ring-protonated and metal-protonated forms were identified. A specific group of protonated forms of the ferrocene and ruthenocene molecules includes four types of structures, *viz.*, ring-protonated (**1a**,**b**) and metal-protonated (**2a**,**b**) structures, transition states of the **1** ⇌ **2** interconversion (**3a**,**b**), as well as ring-protonated structures with the cyclopentadiene ring folded along the C(2)—C(5) line so that the M—H_{endo} interaction is virtually negligible. The latter structures are required for [1,5]-sigmatropic shift of the *exo*-hydrogen atom in the Cp ring to occur. The results obtained were used for the interpretation of the available schemes of electrophilic substitution reactions in metallocenes and of the sigmatropic shift mechanisms.

Key words: density functional theory, regioselectivity of protonation, ferrocene, ruthenocene, osmocene, proton affinity, sigmatropic hydrogen shifts, electrophilic substitution, hydrogen isotope exchange, Onsager principle of microscopic reversibility, rearrangements.

Electrophilic substitution reactions in the ferrocene molecule are of considerable interest not ony due to a great preparative value of this type of reactions. They also place the chemists in a dilemma. Namely, these processes can involve either the initial attack of an electrophile on a carbon atom of the Cp ring or on the metal atom (Scheme 1, routes a_1 and b_1, respectively). Realization of a particular route is determined by a complex balance of

Published in Russian in *Izvestiya Akademii Nauk. Seriya Khimicheskaya,* No. 10, pp. 1749—1756, October, 2002.

1066-5285/02/5110-1900 $27.00

such factors as the nature of the electrophile, the presence of substituents in the ferrocene molecule, and the reaction medium.

Scheme 1

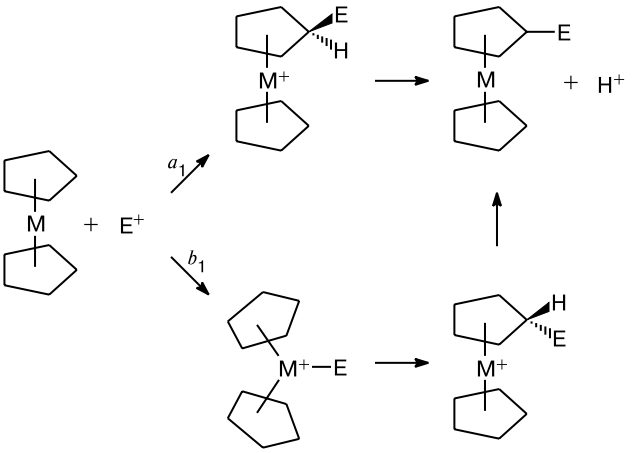

M = Fe, Ru, Os

Elucidation of a particular mechanism (a_1 or b_1) of electrophilic substitution reactions in the ferrocene molecule is hampered by short lifetimes of intermediates, which usually makes spectroscopic detection of these compounds impossible. At the same time, both reaction mechanisms lead to the same stereochemical result. In this connection it is appropriate to remind that the assumptions of particular reaction mechanisms (a_1 [1–6] or b_1 [1,7–9]) based on indirect data were the subject of a discussion in the early studies. Reliable conclusions that acylation of ferrocene follows route a_1 while mercuration of ferrocene follows route b_1 were made based on the results of systematic studies of the reactions of selectively deuterated ferrocenes.[10–12] An investigation of protonation of [1.1]-ferrocenophane provided convincing circumstantial evidence that protonation of ferrocene at the ring occurs faster than at the metal atom.[13]

The aim of this work was to carry out a density functional quantum-chemical study of electrophilic isotope exchange of hydrogen in ferrocene, ruthenocene, and osmocene.

Without regard to the position of the initial attack of $D^+(H^+)$, the electrophilic isotope exchange of hydrogen in metallocenes can occur "symmetrically" (if this position matches that from which H^+ is eliminated) or "asymmetrically" (otherwise). Both these pathways of the electrophilic hydrogen exchange in metallocenes are shown in Scheme 2 taking the initial attack on the metal atom as an example. The "symmetric" process involves the addition of D^+ to the metal atom (Scheme 2, stage a_2), the migration of the deuterium atom from the metal atom to the ring (stage b_2), the [1,5]-sigmatropic shift of the *exo*-hydrogen atom (stage c_2), the migration of the *endo*-hydrogen atom to the metal atom (stage d_2), and the proton elimination (stage e_2). If the reaction follows the "asymmetric" pathway (a_2+b_2+f_2), we deal with proton elimination from the *exo*-position of the ring rather than from the metal atom.

Scheme 2

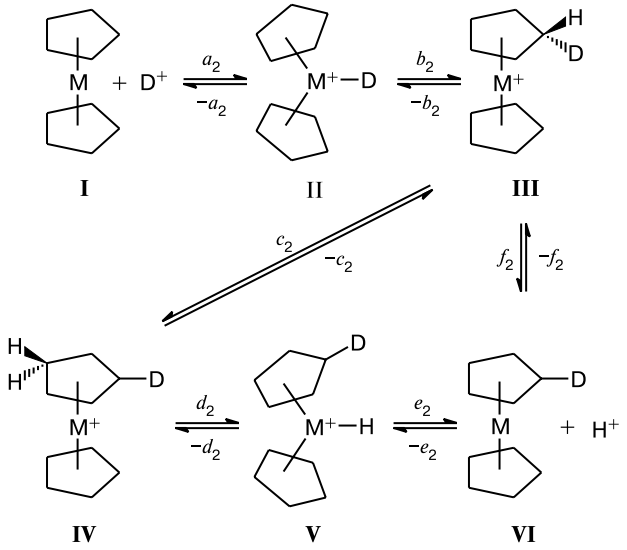

M = Fe, Ru, Os

Electrophilic isotope hydrogen exchange in the ferrocene molecule *via* initial addition of D^+ to the *exo*-position of the Cp ligand is shown in Scheme 3. In this case, the "asymmetric" pathway involves elimination of proton from the metal atom (stages a_3, b_3, and f_3) in the intermediate hydride **V**. The "symmetric" reaction pathway involves migration of the hydride hydrogen atom in complex **V** either to the ring bearing the deuterium atom (stages c_3 and e_3; homoannular substitution), or to the other ring (stages d_3 and e_3; heteroannular substitution).

In this work, the mechanisms of electrophilic isotope exchange of hydrogen shown in Schemes 2 and 3 were analyzed in detail using the density functional approach. Earlier,[14–17] theoretical studies of protonated forms of the ferrocene molecule were performed without analyzing such important stages as the [1,5]-sigmatropic shifts of the *exo*- and *endo*-hydrogen atoms (Scheme 2, stage c_2 and Scheme 3, stage g_3, respectively) while no calculations of the protonation of ruthenocene and osmocene were carried out.

The results of earlier theoretical studies of the protonated ferrocene molecule in the gas phase are contradictory. Despite the fact that calculations[14] were performed both by the Hartree—Fock method and at the second-

Scheme 3

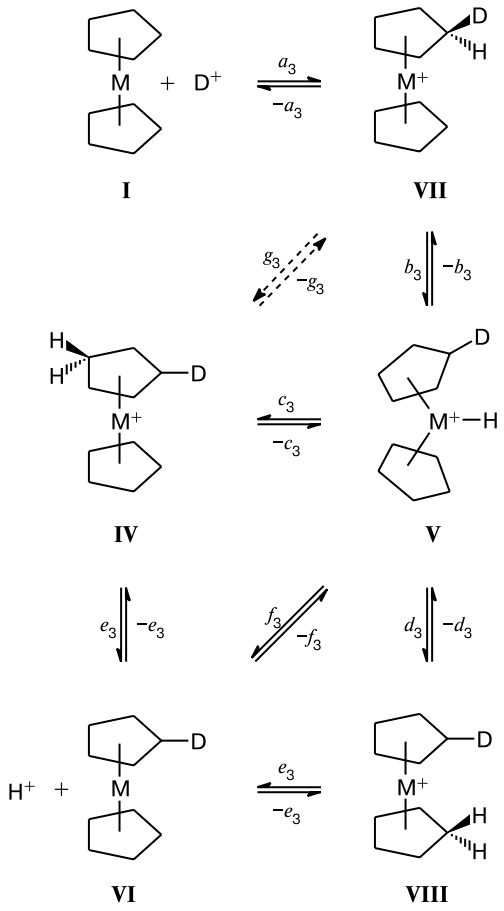

M = Fe, Ru, Os

order Møller—Plesset level of perturbation theory, the conclusions drawn by the authors of this study came under criticism more recently.[15—17] No characteristic points corresponding to proton addition to the *exo*-position of the ring were found on the potential energy surface (PES) of the protonated ferrocene molecule in a density functional study[15] by the LDA and B-PW91 methods. In addition, identification of agostic structures with a H atom located between the metal atom and the Cp ring casts some doubt because of imaginary vibrational frequencies reported for some of them.[15] The geometry of protonated forms of the ferrocene molecule is also still to be clarified since calculations[16] were carried out without geometry optimization. Some detached points to be calculated in this work were chosen based on the results of preliminary calculations[15] and unpublished data.

Calculation Procedure

Calculations of the geometry and electronic structure of protonated forms of the ferrocene, ruthenocene, and osmocene molecules were carried out in the framework of density functional approach with the Becke—Lee—Young—Parr (BLYP) functional.[18,19] Relativistic energy corrections for heavy elements (Ru, Os) were ignored. Analysis of the results of quantum-chemical calculations of heavy-metal organometallic compounds shows that the nonrelativistic approximation is sufficient for correct determination of the energy characteristics of rearrangements (see, *e.g.*, Ref. 20). The geometries of the molecular systems under study were optimized using the Dunning—Hay basis set[21] and the LanL2 pseudopotential.[22] The procedure for location and identification of the transition states (TS) of the interconversions between the metal-protonated and ring-protonated forms (Scheme 3, stages b_2 and d_2, and Scheme 3, stages b_3, c_3, and d_3) and between two ring-protonated forms (stage c_2) involved three steps. First, we calculated an approximate geometry of a corresponding TS by the method of linear synchronous transit (QST2).[23] Then, structure refinement was performed by the quadratic synchronous transit (QST3) method.[22] Finally, we refined the TS structure by the gradient method, analyzed the vibrational frequencies at the saddle point of the PES, and proved the correspondence between the results obtained and the reaction under study by the intrinsic reaction coordinate (IRC) method. Calculations were carried out on CRAY J-90 (National Energy Research Supercomputer Center, Berkeley, California, USA) and SGI Power Challenge computer servers (Environmental Molecular Sciences Laboratory, Pacific Northwest National Laboratories, Richland, Washington, USA) using the GAUSSIAN-98 program suite.[24]

Results and Discussion

Calculations of protonated metallocenes

The results of calculations of the PES fragments of ferrocene are listed in Table 1. Five types of protonated structures were revealed (Scheme 4). The energies of individual structures, the bond lengths, and the bond angles for protonated ferrocene, ruthenocene, and osmocene are listed in Tables 1, 2, and 3, respectively. For protonated ferrocene, the ring-protonated structure **1a** is the most stable. According to our calculations, the proton affinity energy of the ferrocene molecule is 214.2 kcal mol^{-1} (*cf.* 206—213 kcal mol^{-1} for experimental values[25—27]). In molecule **1a**, the C(1) atom has a nearly tetrahedral configuration and is separated from the H_{exo} and H_{endo} atoms by 1.10 and 1.193 Å, respectively. The C(1)—H_{endo} bond is involved in agostic interaction with the iron atom (the Fe—H_{endo} distance is 1.873 Å). The C(2)—C(5) chain fragment is characterized by noticeable alternation of the carbon—carbon bonds, which is typical of η^4-diene complexes.[28] Thus, the cyclopentadiene ring in molecule **1a** is coordinated to the Fe atom in the η^4-,C(1)—H_{endo}-fashion. The geometry of the structure **1a** of protonated ferrocene is much like that found recently;[17] however, no structures similar to **1a** were reported earlier.[15] In the case of **1a** the x_1 and x_2 points correspond to the positions of the centers of gravity of the

protonated and non-protonated five-membered ligands, respectively. The Fe—x_1 distance somewhat exceeds (by 0.013 Å) the Fe—x_2 separation. The x_1—Fe—x_2 angle is about 10° smaller than 180° due to a longer distance between the Cp rings as viewed from the bound "extra" proton. The angle between the π-ligand planes is 8.7°.

Scheme 4

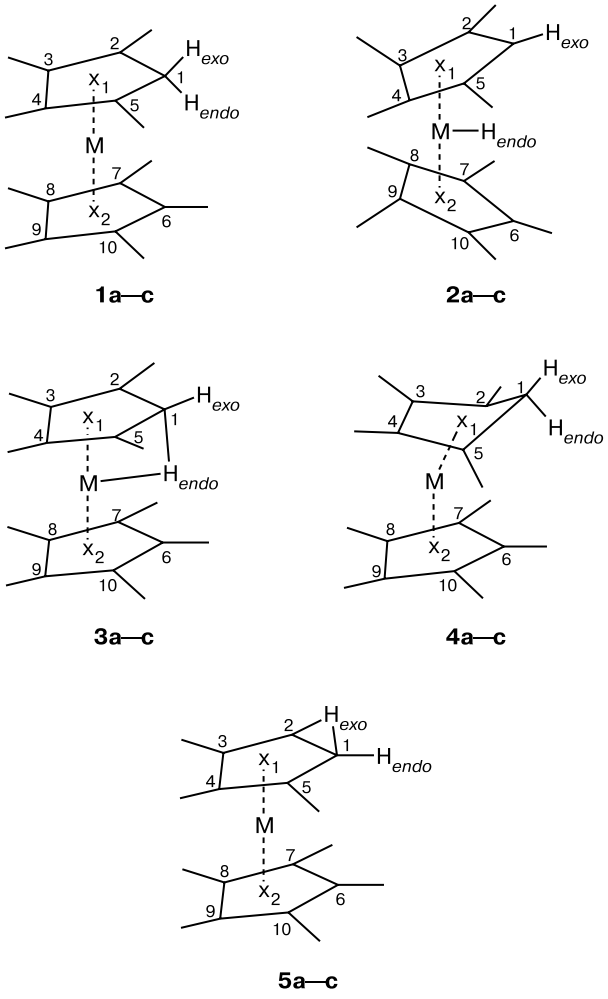

M = Fe (**a**), Ru (**b**), Os (**c**)

The next in stability is structure **2a** of protonated ferrocene. Its energy is 2.7 kcal mol^{-1} (1.9 kcal mol^{-1} with inclusion of zero-point vibrational energy correction) higher than that of **1a**. Similarly to **1a,** optimization led to an eclipsed conformation of **2a**. A feature of this structure is the presence of a hydride hydrogen atom (the Fe—H distance is 1.516 Å), which is at a rather long distance from the C(1) atom (1.960 Å). The cyclopentadienyl rings in **2a** again become equivalent and symmetrically arranged relative to the Fe atom. The angle between the Cp ring planes in **2a** is 13.3°. The geometric parameters of this structure are in agreement with the published results.[15—17] A saddle point corresponding to structure **3a** was also located on the PES of protonated ferrocene. This structure is intermediate between those of **1a** and **2a**. The activation energy of conversion of **1a** into **2a** is 3.0 kcal mol^{-1} (0.3 kcal mol^{-1} for the reverse process).

Table 1. Calculated forms of protonated ferrocene **1a**—**5a***

Parameter	Protonated form				
	1a	**2a**	**3a**	**4a**	**5a**
Bond, *d*/Å					
Fe—C(1)	2.126	2.146	2.110	2.159	2.047
Fe—C(2)	2.146	2.161	2.153	2.002	2.053
Fe—C(3)	2.196	2.159	2.171	2.165	2.130
Fe—C(4)	2.195	2.157	2.172	2.188	2.169
Fe—C(5)	2.143	2.159	2.155	2.081	2.116
C(1)—H_{exo}	1.100	1.090	1.091	1.108	1.318
C(1)—H_{endo}	1.193	1.960	1.666	1.105	1.089
Fe—H_{endo}	1.873	1.516	1.541	2.492	2.787
Fe—X(1)	1.761	1.765	1.757	1.633	1.677
Fe—X(2)	1.748	1.765	1.759	1.746	1.748
C(1)—C(2)	1.524	1.467	1.481	1.591	1.637
C(2)—C(3)	1.427	1.445	1.440	1.435	1.466
C(3)—C(4)	1.464	1.462	1.462	1.464	1.450
C(4)—C(5)	1.427	1.445	1.440	1.432	1.442
C(5)—C(1)	1.524	1.467	1.481	1.546	1.469
Angle, ω/deg					
X(1)—Fe—X(2)	169.5	165.8	167.3	167.8	175.9
C(1)—H_{endo}—Fe	84.7	75.0	82.2	59.8	38.3
−*E*/a.u.	510.5726	510.5683	510.5679	510.5664	510.5343
Δ*E*/kcal mol^{-1}	0.00	2.70	2.95	3.89	24.03
PA/kcal mol^{-1}	214.2	211.5	—	210.3	—

* The total energy of neutral ferrocene molecule calculated by the BLYP/LanL2DZ method is −510.2312 a.u.

All important structural characteristics of **3a**, namely, the Fe—H_{endo} distance (1.541 Å), the C(1)—H_{endo} distance (1.666 Å), and the X_1—Fe—X_2 angle (167.3°) indicate that it is an intermediate between structures **1a** and **2a**. The geometric parameters of **3a** found in this work are close to those reported earlier.[17] At the same time, the C(1)—H_{endo} distance calculated in other studies[15,16] (1.422 and 1.358 Å, respectively) is appreciably different from that obtained from our calculations (1.666 Å) and in a recent study[17] (1.696 Å).

Interconversions between structures **1a**, **2a**, and **3a** correspond to the stages b_2 and d_2 and b_3, c_3 and d_3 (Schemes 2 and 3, respectively). As mentioned above, this work was, in particular, carried out to elucidate the possibility for sigmatropic shifts of the *exo*-hydrogen atoms (stage c_2) to occur. We also located yet another state, **4a**, on the PES of protonated ferrocene. Similarly to **1a**, structure **4a** is also ring protonated but has a different type

of coordination of the cyclopentadiene ligand. In molecule **4a**, the Fe—C(2) and Fe—C(5) distances are shorter than the distances from other carbon atoms of the upper Cp ring to the Fe atom. By drawing a line connecting the C(2) and C(5) atoms we get the folding line of the cyclopentadiene ligand. Because of this, structure **4a** is characterized by two dihedral angles, namely, the angle between the C(2)C(3)C(4)C(5) plane and the C(6)C(7)C(8)C(9)C(10) Cp ring plane (7.4°) and the angle between the C(1)C(2)C(5) plane and the C(6)C(7)C(8)C(9)C(10) Cp ring plane (172.9°). Despite the folding, all C atoms including the most distant C(1), C(3), and C(4) atoms are at bonding distances from the Fe atom. The C(1)—H_{endo}—Fe agostic bond in **4a** is dramatically weakened. This is indicated by nearly equal C(1)—H_{exo} and C(1)—H_{endo} distances (1.108 and 1.105 Å, respectively) and by a rather long Fe—H_{endo} distance (2.492 Å). At the same time, the C(1) atom is at a bonding distance of 2.159 Å from the Fe atom while the Fe—H_{endo} distance is 0.4—0.5 Å shorter than the distances from the Fe atom to the Cp and cyclopentadiene ring protons that are not involved in coordination with the metal atom. This is likely due to the residual agostic interaction. The energy difference between **1a** and **4a** (the energy of **4a** is 3.9 kcal mol^{-1} higher than that of **1a**) is due to weakening of the C(1)—H_{endo}—Fe agostic bond in **4a**. The PES maximum corresponding to the TS of the conversion of **1a** into **4a** is diffuse, so that the activation energy of the reverse conversion of **4a** into **1a** is close to zero. In **4a**, the H_{exo} atom is much more "prepared" for undergoing a [1,5]-sigmatropic shift, since the distances from this atom to the C(2) and C(5) atoms (2.142 Å) are shorter than in **1a** (2.277 Å) and the X_1—C(1)—H_{exo} angle in **4a** (114.6°) is appreciably smaller than in **1a** (143.2°).

In addition to **1a**—**4a**, structure **5a** was located on the PES of protonated ferrocene. Here, the H_{exo} atom is bound to two carbon atoms, C(1) and C(2). The angle between the C(1)—H_{exo}—C(2) plane and the Cp ring plane is 99.57°. The energy of **5a** calculated relative to **1a** is 24.0 kcal mol^{-1}. The lowest vibrational frequency is imaginary (i410 cm^{-1}). Therefore, structure **5a** corresponds to a saddle point. Calculations by the IRC method showed that **5a** is a TS of the [1,5]-sigmatropic hydrogen shift along the perimeter of the Cp ring and connects two equivalent forms **4a**. Structure **1a** is not connected by a reaction channel to TS **5a**. Therefore, if the system initially exists in the form **1a**, it should first pass to the state **4a** to allow the [1,5]-sigmatropic shift along the perimeter of the Cp ring. The activation energy of the [1,5]-sigmatropic shift along the perimeter of the Cp ring is 20.1 kcal mol^{-1}.

We attempted to locate the saddle point of the sigmatropic shift of the H_{endo} atom in structure **1a** from one C atom to the adjacent C atom (Scheme 3, stage g_3). According to calculations, such a saddle point does not exist and the sigmatropic shift of the H_{endo} atom is impossible. Thus, there is only one way for the H atom participating in the agostic bond with the metal atom to migrate to another C atom, which invloves migration toward the metal atom accompanied by cleavage of the C—H bond and formation of a hydride structure followed by migration from the metal atom toward another C atom of any Cp ring.

Five structures, **1b**—**5b**, similar to the ferrocene structures **1a**—**5a** were located on the PES of protonated ruthenocene (Table 2). The calculated proton affinity energy of ruthenocene is 220.3 kcal mol^{-1}, which is ~6 kcal mol^{-1} higher than that of ferrocene (214.2 kcal mol^{-1}). The most stable structure is metal-protonated ruthenocene **2b**, which is isostructural to **2a**. Similarly to protonated ferrocene **2a**, the Cp rings in **2b** are equivalent and symmetrically arranged relative to the metal atom. Structure **2b** is also characterized by the Ru—H bonding distance of 1.608 Å, a long C(1)—H_{endo} distance (2.207 Å), and an angle between the Cp ring planes of 16.7°.

The next in stability form of protonated ruthenocene is ring-protonated structure **1b**, which is isostructural to **1a**. The energy of **1b** is 4.3 kcal mol^{-1} higher than that of **2b** (5.2 kcal mol^{-1} with inclusion of zero-point vibrational

Table 2. Various forms of protonated ruthenocene **1b**—**5b***

Parameter	Protonated form				
	1b	**2b**	**3b**	**4b**	**5b**
Bond, *d*/Å					
Ru—C(1)	2.310	2.320	2.251	2.361	2.150
Ru—C(2)	2.307	2.320	2.300	2.273	2.216
Ru—C(3)	2.345	2.298	2.334	2.439	2.381
Ru—C(4)	2.345	2.298	2.336	2.457	2.393
Ru—C(5)	2.306	2.318	2.301	2.281	2.296
C(1)—H_{exo}	1.102	1.089	1.095	1.145	1.285
C(1)—H_{endo}	1.198	2.207	1.429	1.124	1.145
Ru—H_{endo}	2.022	1.608	1.739	2.572	2.873
Ru—X(1)	1.955	1.950	1.938	1.935	1.915
Ru—X(2)	1.908	1.950	1.927	1.813	1.828
C(1)—C(2)	1.524	1.462	1.500	1.551	1.558
C(2)—C(3)	1.430	1.451	1.438	1.402	1.455
C(3)—C(4)	1.466	1.465	1.464	1.439	1.452
C(4)—C(5)	1.429	1.451	1.438	1.386	1.444
C(5)—C(1)	1.524	1.463	1.500	1.527	1.463
Angle, ω/deg					
X(1)—Ru—X(2)	168.6	164.9	169.6	179.3	172.7
C(1)—H_{endo}—Ru	87.8	73.0	90.0	66.5	41.3
−*E*/a.u.	480.9962	481.0031	480.9949	480.9890	480.9535
Δ*E*/kcal mol^{-1}	4.30	0.00	5.20	10.8	41.2
PA/kcal mol^{-1}	216.0	220.3	—	209.5	—

* The total energy of neutral ruthenocene molecule calculated by the BLYP/LanL2DZ method is −480.6521 a.u.

energy correction). Structure **1b** exhibits all features of the η^4,C(1)—H_{endo}-coordination of the cyclopentadiene ring to the Ru atom, that is, tetrahedral configuration of the C(1) atom, elongation (by 0.096 Å) of the C—H_{endo} bond as compared to the C—H_{exo} bond, the Ru—H distance of 2.022 Å, and alternation of the carbon-carbon bonds in the C(2)—C(5) chain fragment. The angle between the Cp ring planes is 11.3°. Thus, for ferrocene and ruthenocene the angles between the Cp ring planes in the ring-protonated and metal-protonated forms differ insignificantly, which is consistent with the results of recent quantum-chamical calculations of protonated ferrocene.[17]

The saddle point **3b** located on the PES corresponds to the TS of a proton migration in **2b** (**2b** → **1b**). The activation energy of this transformation was found to be 5.2 kcal mol^{-1}. Structure **4b** of protonated ruthenocene with the cyclopentadiene ring folded along the C(2)—C(5) line is isostructural to form **4a** of protonated ferrocene. By drawing a line connecting the C(2) and C(5) atoms in molecule **4b** we get the folding line of the cyclopentadiene ring; the Ru—C(2) and Ri—C(5) distances are shorter than the distances from other carbon atoms of the upper cyclopentadiene ring to the Ru atom. Similarly to the isostructural **4a**, two dihedral angles in protonated ruthenocene **4b** characterize the folding of the cyclopentadiene ring. These are the angle between the C(2)C(3)C(4)C(5) plane and the C(6)C(7)C(8)C(9)C(10) Cp ring plane (5.9°) and the angle between the C(1)C(2)C(5) plane and the C(6)C(7)C(8)C(9)C(10) Cp ring plane (172.0°). The C(1)—H_{endo}—Ru agostic bond in structure **4b** is also weakened, as is the case of **4a**. This manifests itself in shortening of the C(1)—H_{endo} distance and in lengthening of the Ru—H_{endo} distance. However, the Ru—C(1) bonding distance and the shortened Ru—H_{endo} distance (on the average, by 0.56 Å) compared to the distances from the Ru atom to the protons at the C(2)—C(9) atoms that are not involved in coordination with the metal atom can be interpreted as an indication of the residual agostic C(1)—H_{endo} interaction with the metal atom. The energy of structure **4b** is 10.8 kcal mol^{-1} higher than that of **2b**. Structure **5b** is a transition state of the [1,5]-sigmatropic shift along the perimeter of the cyclopentadiene ring. The calculated activation energy of such a migration (41.2 kcal mol^{-1} relative to **2b**) is much higher than the activation barrier to the analogous process in protonated ferrocene.

Among protonated metallocenes of iron subgroup elements, osmocene occupies a special position. Only a stationary point corresponding to structure **2c** was located on the PES of protonated osmocene. The principal characteristics of this structure are listed in Table 3. This structure is characterized by the presence of a hydride hydrogen atom and an Os—H distance of 1.635 Å. The cyclopentadienyl rings in **2c** are equivalent and symmetrically arranged with respect to the Os atom. The angle between the Cp ring planes in **2c** is 19.6°. The calculated proton affinity energy of osmocene is 229.7 kcal mol^{-1}.

Table 3. Geometric parameters of protonated osmocene **2c***

Parameter	Value	Parameter	Value
Bond, *d*/Å		Bond, *d*/ÅÅ	
Os—C(1)	2.336	C(2)—C(3)	1.457
Os—C(2)	2.322	C(3)—C(4)	1.469
Os—C(3)	2.285	C(4)—C(5)	1.457
Os—C(4)	2.285	C(5)—C(1)	1.463
Os—C(5)	2.322	Angle, ω/deg	
C(1)—H_{exo}	1.089	X(1)—Os—X(2)	163.3
C(1)—H_{endo}	2.257	C(1)—H_{endo}—Ru	71.77
Os—H_{endo}	1.635	−*E*/a.u.	478.1644
Os—X(1)	1.947	*PA*/kcal mol^{-1}	229.6
Os—X(2)	1.947		
C(1)—C(2)	1.463		

* The total energy of neutral osmocene molecule calculated by the BLYP/LanL2DZ method is –477.7984 a.u.

Analysis of electrophilic isotope exchange of hydrogen in metallocenes

Based on the results of our calculations, we can draw some conclusions concerning electrophilic isotope exchange of hydrogen in ferrocene and ruthenocene.

1. For the addition of D^+ (H^+) to metallocenes to result in D/H isotope exchange in the Cp rings rather than be a simple acid—base equilibrium a particular reaction stage must involve at least one migration of the H (D) atom from the metal atom to the ring (in the case of attack on the metal atom, Scheme 2) or from the ring to the metal atom if the ring is initially attacked (Scheme 3).

If an "external" D^+ (H^+) attacks the ring, the isotope exchange can occur without intermediate formation of hydride forms **2** from **1** only if the reaction pathway involves either an elimination of the *endo*-proton from the ring-protonated structures **1** (structures III, IV, VII, and VIII in Schemes 2 and 3) or a sigmatropic shift of the *endo*-H atom along the perimeter of the ring followed by elimination of the *exo*-proton (Scheme 3, route $a_3 + g_3 + e_3$). As mentioned above, both conditions cannot be met since the *endo*-hydrogen atom in structure **1** is involved in agostic interaction with the metal atom and the [1,5]-sigmatropic shift of this atom is impossible. Therefore, the occurrence or absence of electrophilic isotope exchange of hydrogen will be determined by the energy difference between structures **1** and **2** and by the energy barrier separating them. The smaller the energy difference between **1** and **2** and the lower the activation barrier to interconversion between them, the easier the electrophilic isotope exchange of hydrogen. If in solution one of these structures will be much more stable than the

other (*i.e.*, if the change in the free energy will be sufficiently large), electrophilic H/D isotope exchange in metallocenes will not occur at all or will occur very slowly.

2. Since, according to calculations, the smallest energy difference between structures **1** and **2** and the lowest energy barrier separating them were found for protonated ferrocene, electrophilic H/D isotope exchange must occur most easily in ferrocene. On going down the group of the periodic table the proton affinity energies of metallocenes Cp_2M increase (our calculations gave 214.2, 220.3, and 229.7 kcal mol^{-1} for M = Fe, Ru, and Os, respectively) and so do the stabilities of the hydride structures $[Cp_2MH]^+$ relative to the ring-protonated forms $[(\eta^5\text{-Cp})M(\eta^4, C(1)—H_{endo}—C_5H_6)]^+$. For M = Ru, the hydride structure **2b** is more stable than the ring-protonated form **1b**; however, the energy difference between them is insufficient to prevent the equilibration of both forms in solution. For M = Os, the energy difference between the metal-protonated and ring-protonated forms of osmocene is so large that no point corresponding to the latter structure was located on the PES of protonated osmocene. Therefore, electrophilic H/D isotope exchange in osmocene is hardly probable and no information on this process in this compound and its derivatives is available. Thus, the easiness of electrophilic H/D exchange depends on the nature of the metal atom. This is in agreement with the fact that the most stable agostic structures are formed by the first-row transition metal complexes.[29] On going down the groups of the periodic table the relative stability of the oxidative addition products of the C—H agostic bond to the metal atom increases due to weakening of the agostic interaction and to strengthening of the metal—hydrogen bond.[30]

3. The results obtained suggest that the allowed routes of electrophilic H/D exchange in Schemes 2 and 3 include (i) "asymmetric" substitution (Scheme 2, route $a_2 + b_2 + f_2$) if the reaction begins with attack on the metal atom and (ii) "symmetric homoannular" (Scheme 3, route $a_3 + b_3 + c_3 + e_3$), (iii) "symmetric heteroannular" substitution (Scheme 3, route $a_3 + b_3 + d_3 + e_3$), and (iv) "asymmetric" substitution (Scheme 3, route $a_3 + b_3 + f_3$) if the ring is initially attacked. Thus, of the reaction routes shown in Schemes 2 and 3 only the "symmetric" substitution beginning with attack on the metal atom (Scheme 2, route $a_2 + b_2 + c_2 + d_2 + e_2$) can be considered forbidden. This process should be rather slow, since in this case the rate-limiting step ([1,5]-sigmatropic shift of the H_{exo} atom, stage c_2) is characterized by a high activation barrier (24 kcal mol^{-1} relative to **1a**). The proportion of molecules following this route in both directions is negligible compared with the above-mentioned "allowed" routes. In the framework of the principle of microscopic reversibility one can expect that in the case of protonated ferrocene the fractions of the molecules that followed the "allowed" routes $a_2 + b_2 + f_2$, $a_3 + b_3 + c_3 + e_3$, $a_3 + b_3 + d_3 + e_3$, and $a_3 + b_3 + f_3$, will be comparable. The same routes are also allowed for protonated ruthenocene; however, here the proportion of the molecules that followed the $a_2 + b_2 + f_2$ route beginning with attack on the metal atom should be much larger than the proportion of the molecules that follow the ring attack route (Scheme 3, routes $a_3 + b_3 + c_3 + e_3$, $a_3 + b_3 + d_3 + e_3$, and $a_3 + b_3 + f_3$). By analogy with protonated ferrocene in the case of protonated ruthenocene the "symmetric" route (Scheme 2, route $a_2 + b_2 + c_2 + d_2 + e_2$) beginning with attack on the metal atom should be considered forbidden, since the kinetic barrier to the rate-limiting step ([1,5]-sigmatropic shift of the H_{exo} atom in structure **1b**) is much higher than in the case of analogous iron structure (37 and 24 kcal mol^{-1}, respectively).

By and large, these conclusions are in agreement with the reported data on protonated ferrocenes and ruthenocenes and on the occurrence of electrophilic H/D exchange in them. These metallocenes are weak bases with two basicity centres, namely, the metal atom and the Cp ring. Ferrocene forms complexes with weak proton donors (chloroform, phenylacetylene, phenol) and proton donors of moderate strength (CF_3COOH, CCl_3COOH). In these complexes, the proton donor is bound to the Cp ring by a hydrogen bond. These conslusions are based on the results of (i) experimental studies using IR spectroscopy[31] and electronic spectroscopy[32] and (ii) analysis of the changes in the chemical shifts of the NMR signals of proton donors in the presence of ferrocene and of the singlet of the ferrocene Cp protons in the presence of proton donors.[33,34] In contrast to ferrocene, the reactions of ruthenocene and osmocene with the same proton donors result in the formation of a hydrogen bond with the metal atom.[35,36] A number of systems (ferrocene in neat F_3CCOOD, ferrocene in solutions of D_3PO_4, F_3CCOOD, and Cl_3CCOOD in organic solvents; ruthenocene[29] in neat F_3CCOOD and in Cl_3CCOOD in organic solvents) is characterized by rather fast electrophilic H/D exchange.[37]

Protonated forms of ferrocene and ruthenocene with the lifetimes sufficiently long to be identified by ^{1}H NMR spectroscopy were only detected in strong acids where the acid anion is either a weaker base than metallocenes or is comparable with them in basicity. According to calculations, ruthenocene forms hydride structures more easily. In $BF_3 \cdot H_2O$ solutions, ruthenocene exists only as a pure hydride form $[Cp_2RuH]^+$ (**2b**), which can be detected by the appearance of singlets of the cyclopentadienyl and hydride protons with a characteristic signal intensity ratio of 10 : 1 in the ^{1}H NMR spectra. The ^{1}H NMR spectra of ferrocene solutions in $BF_3 \cdot H_2O$ exhibit doublet signals of the Cp ring protons and an undecet ($J_{H,Cp}$ = 1.75 Hz) of the hydride ligand,[13] which can be explained by fast (in the NMR time scale) interconversion between the hydride $[Cp_2FeH]^+$ (**2a**) and ring-protonated (**1a**) isomers.

The contribution of the latter structure is detected by the appearance of the spin—spin coupling between the cyclopentadienyl and hydride hydrogen atoms. Protonated ferrocene exists as a pure hydride form **2a** only under unusual conditions (in a solution of the superacid HSO_3F : SO_2ClF, 1 : 10 by volume, at −125 °C).[17] The spin—spin coupling between the hydride and Cp ring protons in **2a** was not detected. In this case electrophilic H/D exchange does not occur. Finally, all things being equal, the rate of electrophilic H/D exchange in ruthenocene is lower than in ferrocene.[37]

Based on the results obtained, we can draw the following conclusions.

1. Five isostructural forms were located on the PES of protonated ferrocene and ruthenocene. They correspond to the ring-protonated (**1a**, **1b**) and metal-protonated structures (**2a**, **2b**), the transition states of interconversions between them (**3a**, **3b**), the cyclopentadiene structures folded along the C(2)—C(5) line (**4a**, **4b**), and, finally, the transition states of [1,5]-sigmatropic shift of the *exo*-hydrogen atom (**5a**, **5b**). The ring-protonated forms **1a** and **1b** are characterized by the presence of the C(1)—H_{endo}—M agostic bond that is cleaved on going to the folded cyclopentadiene complexes **4a** and **4b**.

2. On going down the group of the periodic table from M = Fe to M = Ru and Os the hydride structures, $[Cp_2MH]^+$, become more stable relative to the ring-protonated forms, $[(\eta^5\text{-Cp})M(\eta^2\text{-C(1)}H_{endo}\text{:}\eta^4\text{-}C_5H_6)]^+$. For M = Fe, the ring-protonated form **1a** is more stable than hydride **2a** in the gas phase; however, the energy difference between them is very small and the energy barrier separating both structures is the lowest. If M = Ru, the hydride **2b** is more stable than the ring-protonated form **1b**. Here, the energy difference between the isomeric forms and the kinetic barrier separating them are somewhat larger than in the case of **1a** and **2a**. For M = Os, protonated osmocene can exist in the gas phase only as hydride **2c**.

3. Electrophilic H/D exchange in metallocenes can occur only *via* an interconversion between the ring-protonated (**1a**, **1b**) and metal-protonated (**2a**, **2b**) structures as the key intermediates. Its rate must decrease with an increase in the kinetic barrier and the energy difference between the isomeric pairs (**1a**, **2a**) and (**1b**, **2b**). This is consistent with the higher rate of H/D exchange in ferrocene compared to ruthenocene and the absence of such a process in protonated osmocene.

4. Electrophilic H/D exchange in ferrocene and ruthenocene following the routes involving [1,5]-sigmatropic shifts of the *exo*-hydrogen atoms (Scheme 2, route $a_2 + b_2 + c_2 + d_2 + e_2$) is forbidden. Other reaction pathways beginning with attack on both the metal atom (Scheme 2, route $a_2 + b_2 + f_2$) and the Cp ring (Scheme 3, routes $a_3 + b_3 + c_3 + e_3$, $a_3 + b_3 + d_3 + e_3$ and $a_3 + b_3 + f_3$), must be allowed.

The calculations were carried out by Yu. A. Borisov at Associated Western Universities Inc. Faculty Fellowship on behalf of the Environmental Molecular Sciences Laboratory, Pacific Northwest National Laboratories (Richland, Washington, USA). The authors express their gratitude to the Pacific Northwest National Laboratories (Richland, Washington, USA) for providing the time on the CRAY J-90 supercomputer (National Energy Research Supercomputer Center, Berkeley, California, USA) under Contract No. DE-AC06-76RLO 1830 with the U.S. Department of Energy) and on SGI Power Challenge Computer Servers (Environmental Molecular Sciences Laboratory, Pacific Northwest National Laboratories, Richland, Washington, USA).

This work was carried out with partial financial support of the Russian Foundation for Basic Research (Project No. 99-03-33060).

References

1. W. E. Watts, in *Comprehensive Organometallic Chemistry*; Eds. G. Wilkinson, F. G. A. Stone, and E. N. Abel, Pergamon, New York, 1982, **8**, Ch. 59, 1019.
2. J. H. Richards, *Abstr. 135-th Meeting Am. Chem. Soc.*, April 1959, 86.
3. R. A. Benkeser, Y. Nagai, and J. Hooz, *J. Am. Chem. Soc.*, 1964, **86**, 3742.
4. K. L. Rinehart, D. E. Bublitz, and D. H. Gustafson, *J. Am. Chem. Soc.*, 1963, **85**, 970.
5. M. Rosenblum and F. W. Abbate, *J. Am. Chem. Soc.*, 1966, **88**, 4178.
6. J. C. Ware and T. G. Traylor, *Tetrahedron Lett.*, 1965, 1295.
7. M. Rosenblum, J. O. Santer, and W. G. Howells, *J. Am. Chem. Soc.*, 1963, **85**, 1450.
8. T. J. Curphey, J. O. Santer, and M. Rosenblum, *J. Am. Chem. Soc.*, 1960, **82**, 5249.
9. E. G. Perevalova and T. V. Nikitina, in *Organometallic Reactions*, Eds. E. I. Becker and M. Tsutsui, Wiley-Interscience, New York, 1972, **4**, 175.
10. A. F. Cunningham, *J. Am. Chem. Soc.*, 1991, **113**, 4864.
11. A. F. Cunningham, *Organometallics*, 1994, **13**, 2480.
12. A. F. Cunningham, *Organometallics*, 1997, **16**, 1114.
13. U. T. Mueller-Westerhoff, G. F. Haas, G. F. Swiegers, and T. K. Leipert, *J. Organomet. Chem.*, 1994, **472**, 229.
14. M. L. McKee, *J. Am. Chem. Soc.*, 1993, **115**, 2818.
15. M. J. Mayor-Lopez, J. Weber, B. Mannfors, and A. F. Cunningham, *Organometallics*, 1998, **17**, 4983.
16. M. J. Mayor-Lopez, H. P. Luthi, H. Koch, P. Y. Morgantini, and J. Weber, *J. Chem. Phys.*, 2000, **113**, 8009.
17. A. Karlsson, A. Broo, and P. Ahlberg, *Can. J. Chem.*, 1999, **77**, 628.
18. A. D. Becke, *J. Chem. Phys.*, 1993, **98**, 5648.
19. C. Lee, W. Yang, and R. G. Parr, *Phys. Rev.*, *B*, 1988, **150**, 785.
20. Niu Shuqiang and M. B. Hall, *Chem. Rev.*, 2000, **100**, 353.
21. T. H. Dunning, Jr. and P. J. Hay, in *Modern Theoretical Chemistry*, Ed. H. F. Schaefer III, Plenum, New York, 1976, 1.
22. P. J. Hay and W. R. Wadt, *J. Chem. Phys.*, 1985, **82**, 270.

23. C. Peng and H. B. Schlegel, *Israel J. Chem*., 1993, **33**, 449.
24. GAUSSIAN 98, Revision A. 5, Gaussian, Inc., Pittsburgh PA, 1998.
25. M. S. Foster and J. L. Beuchamp, *J. Am. Chem. Soc*., 1975, **97**, 4814.
26. M. G. Ikonomou, J. Sunner, and P. Kebarle, *J. Phys. Chem*., 1988, **92**, 6308.
27. M. Meot-Ner (Mautner), *J. Am. Chem. Soc*., 1989, **111**, 2830.
28. D. M. P. Mingos, in *Comprehensive Organometallic Chemistry*, Eds. G. Wilkinson, F. G. A. Stone, and E. N. Abel, Pergamon: New York, 1982, **3**, Ch. 19.4.5.
29. R. H. Crabtree and D. G. Hamilton, *Adv. Organomet. Chem*., 1968, **28**, 299.
30. J. A. M. Simões and J. L. Beauchamp, *Chem. Rev*., 1990, **90**, 629.
31. L. M. Epshtein, L. D. Ashkinadze, S. O. Rabicheva, and L. A. Kazitsyna, *Doklady Akad. Nauk SSSR*, 1970, **190**, 128 [*Dokl. Chem*., 1970 (Engl. Transl.)].
32. B. Floris, G. Illuminati, and G. Ortaggi, *Tetrahedron Lett*., 1972, 269.
33. G. Gerichelli, G. Illuminati, G. Ortaggi, and A. M. Giuliani, *J. Organomet. Chem*., 1977, **127**, 357.
34. T. E. Bitterwolf and A. C. Ling, *J. Organomet. Chem*., 1972, **40**, 197.
35. L. M. Epshtein and E. S. Shubina, *Metalloorg. Khim*., 1992, **5**, 61 [*Organomet. Chem. USSR*, 1992, **5** (Engl. Transl.)].
36. L. M. Epstein, A. N. Krylov, and E. S. Shubina, *J. Mol. Struct*., 1999, **322**, 345.
37. V. N. Setkina and D. N. Kursanov, *Usp. Khim*., 1968, **37**, 1729 [*Russ. Chem. Rev*., 1968, **37** (Engl. Transl.)].

Recieved October 4, 2001;
in revised form July 3, 2002